

# Higher-order interactions shape collective dynamics differently in hypergraphs and simplicial complexes

Yuanzhao Zhang,<sup>1,\*</sup> Maxime Lucas,<sup>2,3,\*</sup> and Federico Battiston<sup>4</sup>

<sup>1</sup>*Santa Fe Institute, 1399 Hyde Park Road, Santa Fe, NM 87501, USA*

<sup>2</sup>*ISI Foundation, Via Chisola 5, 10126 Torino, Italy*

<sup>3</sup>*CENTAI Institute, 10138 Torino, Italy*

<sup>4</sup>*Department of Network and Data Science, Central European University, 1100 Vienna, Austria*

Higher-order networks have emerged as a powerful framework to model complex systems and their collective behavior. Going beyond pairwise interactions, they encode structured relations among arbitrary numbers of units through representations such as simplicial complexes and hypergraphs. So far, the choice between simplicial complexes and hypergraphs has often been motivated by technical convenience. Here, using synchronization as an example, we demonstrate that the effects of higher-order interactions are highly representation-dependent. In particular, higher-order interactions typically enhance synchronization in hypergraphs but have the opposite effect in simplicial complexes. We provide theoretical insight by linking the synchronizability of different hypergraph structures to (generalized) degree heterogeneity and cross-order degree correlation, which in turn influence a wide range of dynamical processes from contagion to diffusion. Our findings reveal the hidden impact of higher-order representations on collective dynamics, highlighting the importance of choosing appropriate representations when studying systems with nonpairwise interactions.

## I. INTRODUCTION

For the past three decades, networks have been successfully used to model complex systems with many interacting units. In their traditional form, networks only encode pairwise interactions [1, 2]. Growing evidence, however, suggests that a node may often experience the influence of multiple other nodes in a nonlinear fashion and that such higher-order interactions cannot be decomposed into pairwise ones [3–7]. Examples can be found in a wide variety of domains including human dynamics [8], collaborations [9], ecological systems [10], and the brain [11, 12]. Higher-order interactions not only impact the structure of these systems [13–21], they also often reshape their collective dynamics [22–27]. Indeed, they have been shown to induce novel collective phenomena, such as explosive transitions [28], in a variety of dynamical processes including diffusion [29, 30], consensus [31, 32], spreading [33–35], and evolution [36].

Despite many recent theoretical advances [37–42], little attention has so far been given to how higher-order interactions are best represented [43]. There are two mathematical frameworks that are most commonly used to model systems with higher-order interactions: hypergraphs [44] and simplicial complexes [45]. In most cases, the two representations have been used interchangeably and the choice for one or the other often appears to be motivated by technical convenience. For example, topological data analysis [46] and Hodge decomposition [47] require simplicial complexes. Here, we ask: Are there hidden consequences of choosing one higher-order representation over the other that could significantly impact the collective dynamics?

Answering this question is important given that, currently, reliable real-world hypergraph data are still scarce (with most existing ones concentrated in social systems), especially for complex dynamical systems such as the brain. For these systems, in order to study the effect of higher-order interactions, we have to start from data on pairwise networks and infer the potential nonpairwise connections [48]. A popular practice is to assume homophily between pairwise and nonpairwise interactions (e.g., by attaching three-body interactions to closed triangles in the network), effectively choosing simplicial complex as the higher-order representation. However, if different ways of adding hyperedges can fundamentally change the collective dynamics, then conclusions drawn from investigating a single higher-order representation could be misleading.

To explore this issue, we focus on synchronization—a paradigmatic process for the emergence of order in populations of interacting entities. It underlies the function of many natural and man-made systems [49, 50], from circadian clocks [51] and vascular networks [52] to the brain [53]. Nonpairwise interactions arise naturally in synchronization from the phase reduction of coupled oscillator populations [54–58]. A key question regarding higher-order interactions in this context is: When do they promote synchronization? Recently, hyperedge-enhanced synchronization has been observed for a wide range of node dynamics [39, 41, 59–61]. It is thus tempting to conjecture that nonpairwise interactions synchronize oscillators more efficiently than pairwise ones. This seems physically plausible given that higher-order interactions enable more nodes to exchange information simultaneously, thus allowing more efficient communication and ultimately leading to enhanced synchronization performance.

In this Article, we show that whether higher-order interactions promote or impede synchronization is highly

---

\* Y.Z. and M.L. contributed equally to this work.

representation-dependent. In particular, through a rich-get-richer effect, higher-order interactions consistently destabilize synchronization in simplicial complexes. On the other hand, higher-order interactions tend to stabilize synchronization in a broad class of hypergraphs, including random hypergraphs and semi-structured hypergraphs constructed from synthetic networks as well as brain connectome data. Offering a theoretical underpinning for the representation-dependent synchronization performance, we link the opposite trends to the different higher-order degree heterogeneities under the two representations. Furthermore, we investigate the impact of cross-order degree correlations for different families of hypergraphs. Since degree heterogeneity and degree correlation play a key role not only in synchronization but also in other dynamical processes such as diffusion and contagion, the effect of higher-order representations discovered here is likely to be crucial in complex systems beyond coupled oscillators.

## II. RESULTS

### A. Higher-order interactions hinder synchronization in simplicial complexes but facilitate it in random hypergraphs

To isolate the effect of higher-order interactions from node dynamics, we consider a simple system consisting of  $n$  identical phase oscillators [39], whose states  $\boldsymbol{\theta} = (\theta_1, \dots, \theta_n)$  evolve according to

$$\begin{aligned} \dot{\theta}_i = & \omega + \frac{\gamma_1}{\langle k^{(1)} \rangle} \sum_{j=1}^n A_{ij} \sin(\theta_j - \theta_i) \\ & + \frac{\gamma_2}{\langle k^{(2)} \rangle} \sum_{j,k=1}^n \frac{1}{2} B_{ijk} \frac{1}{2} \sin(\theta_j + \theta_k - 2\theta_i). \end{aligned} \quad (1)$$

Equation (1) is a natural generalization of the Kuramoto model [62] that includes interactions up to order two (i.e., three-body interactions). The oscillators have natural frequency  $\omega$  and the coupling strengths at each order are  $\gamma_1$  and  $\gamma_2$ , respectively. The adjacency tensors determine which oscillators interact:  $A_{ij} = 1$  if nodes  $i$  and  $j$  have a first-order interaction, and zero otherwise. Similarly,  $B_{ijk} = 1$  if and only if nodes  $i$ ,  $j$  and  $k$  have a second-order interaction. All interactions are assumed to be unweighted and undirected. The (generalized) degrees are given by  $k_i^{(1)} = \sum_{j=1}^n A_{ij}$  and  $k_i^{(2)} = \frac{1}{2} \sum_{j,k=1}^n B_{ijk}$ , respectively. Here, we normalize  $B_{ijk}$  by a factor of two to avoid double counting the same 2-simplex.

Following Refs. [59, 63], we set

$$\gamma_1 = 1 - \alpha, \quad \gamma_2 = \alpha, \quad \alpha \in [0, 1]. \quad (2)$$

The parameter  $\alpha$  controls the relative strength of the first- and second-order interactions, from all first-order ( $\alpha = 0$ ) to all second-order ( $\alpha = 1$ ), allowing us to keep

the total coupling budget constant and compare the effects of pairwise and nonpairwise interactions fairly. In addition, we normalize each coupling strength by the average degree of the corresponding order,  $\langle k^{(\ell)} \rangle$ .

Finally, we normalize the second-order coupling function by an additional factor of two so that each interaction contributes to the dynamics with an equal weight regardless of the number of oscillators involved. Note that another interaction term of the form  $\sin(2\theta_j - \theta_k - \theta_i)$  appears naturally in other formulations obtained from phase reduction [54, 55, 57]. This type of terms was shown to be dynamically equivalent to that in Eq. (1) when considering the linearized dynamics around full synchrony [39]. Indeed, they yield the same contribution to the Laplacian as long as they are properly normalized by the factor in front of  $\theta_i$ , as we did.

Synchronization,  $\theta_i = \theta_j$  for all  $i \neq j$ , is a solution of Eq. (1) and we are interested in the effect of  $\alpha$  on its stability. The system allows analytical treatment following the multiorder Laplacian approach introduced in Ref. [39]. We define the second-order Laplacian as

$$L_{ij}^{(2)} = k_i^{(2)} \delta_{ij} - \frac{1}{2} A_{ij}^{(2)}, \quad (3)$$

which is a natural generalization of the graph Laplacian  $L_{ij}^{(1)} \equiv L_{ij} = k_i \delta_{ij} - A_{ij}$ . Here, we used the generalized degree  $k_i^{(2)} = \frac{1}{2} \sum_{j,k=1}^n B_{ijk}$  and the second-order adjacency matrix  $A_{ij}^{(2)} = \sum_{k=1}^n B_{ijk}$ .

Using the standard linearization technique, the evolution of a generic small perturbation  $\delta\boldsymbol{\theta} = (\delta\theta_1, \dots, \delta\theta_n)$  to the synchronization state can now be written as

$$\delta\dot{\theta}_i = - \sum_{j=1}^n L_{ij}^{(\text{mul})} \delta\theta_j, \quad (4)$$

in which the multiorder Laplacian

$$L_{ij}^{(\text{mul})} = \frac{1 - \alpha}{\langle k^{(1)} \rangle} L_{ij}^{(1)} + \frac{\alpha}{\langle k^{(2)} \rangle} L_{ij}^{(2)}. \quad (5)$$

We then sort the eigenvalues of the multiorder Laplacian  $\Lambda_1 \geq \Lambda_2 \geq \dots \geq \Lambda_{n-1} \geq \Lambda_n = 0$ . The Lyapunov exponents of Eq. (4) are simply the opposite of those eigenvalues. We set  $\lambda_i = -\Lambda_{n+1-i}$  so that  $0 = \lambda_1 \geq \lambda_2 \geq \dots \geq \lambda_n$ . The second Lyapunov exponent  $\lambda_2 = -\Lambda_{n-1}$  determines synchronization stability:  $\lambda_2 < 0$  indicates stable synchrony, and larger absolute values indicate a quicker recovery from perturbations.

We start by showing numerically the effect of  $\alpha$  (the proportion of coupling strength assigned to second-order interactions) on  $\lambda_2$ . By considering the two classes of structures shown in Fig. 1: simplicial complexes and random hypergraphs, we find that these two canonical constructions exhibit opposite trends.

The construction of random hypergraphs is determined by wiring probabilities  $p_d$ : a  $d$ -hyperedge is created between any  $d + 1$  of the  $n$  nodes with probability  $p_d$  [64].

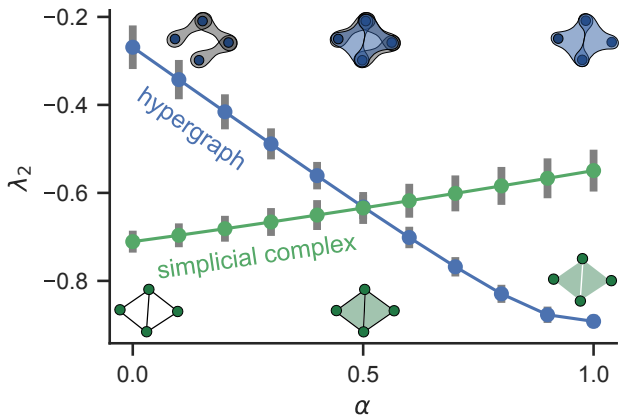


FIG. 1. **Synchronization is enhanced by higher-order interactions in random hypergraphs but is impeded in simplicial complexes.** The maximum transverse Lyapunov exponent  $\lambda_2$  is plotted against  $\alpha$  for random hypergraphs (blue) and simplicial complexes (green). As  $\alpha$  is increased, the coupling goes from first-order-only ( $\alpha = 0$ ) to second-order-only ( $\alpha = 1$ ). Each point represents the average over 50 independent hypergraphs or simplicial complexes with  $n = 100$  nodes. The error bars represent standard deviations. We set  $p = p_\Delta = 0.1$  for random hypergraphs and  $p = 0.5$  for simplicial complexes.

Here, we focus on  $d$  up to 2, so the random hypergraphs are constructed by specifying  $p_1 = p$  and  $p_2 = p_\Delta$ . Simplicial complexes are special cases of hypergraphs and have the additional requirement that if a second-order interaction  $(i, j, k)$  exists, then the three corresponding first-order interactions  $(i, j)$ ,  $(i, k)$ , and  $(j, k)$  must also exist. We construct simplicial complexes by first generating an Erdős–Rényi graph with wiring probability  $p$ , and then adding a three-body interaction to every three-node clique in the graph (also known as flag complexes).

Figure 1 shows that higher-order interactions impede synchronization in simplicial complexes, but improve it in random hypergraphs. For simplicial complexes, the maximum transverse Lyapunov exponent  $\lambda_2$  increases with  $\alpha$  for all  $p$  (data shown for  $p = 0.5$  in Fig. 1). For random hypergraphs, the opposite monotonic trend holds for  $p \simeq p_\Delta$ . For  $p$  significantly larger than  $p_\Delta$ , the curve becomes U-shaped, with the minimum at an optimal  $0 < \alpha^* < 1$ , as shown in Fig. 2.

Our findings also hold when we control the simplicial complex and random hypergraph to have the same number of connections (see Supplementary Fig. S1) and for simplicial complexes obtained by filling empty triangles in random hypergraphs [33], as shown in Supplementary Fig. S2. We note that instead of filling every pairwise triangle in the graph, we can also fill the triangles with a certain probability. As long as the probability is not too close to zero, the results in the paper remain the same (see Supplementary Fig. S3). One can also construct simplicial complexes from structures other than Erdős–Rényi graphs, such as small-world networks [65]. The results above are robust to the choice of different network struc-

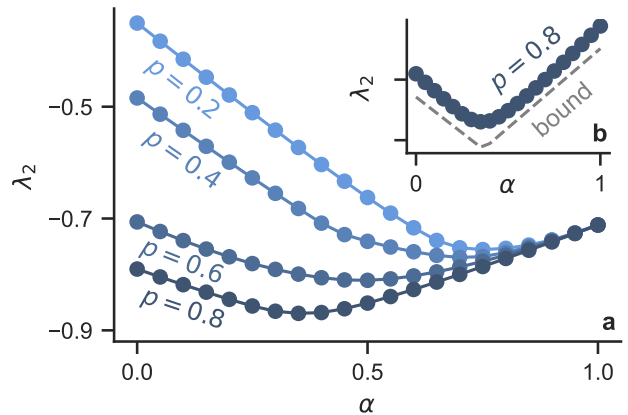


FIG. 2. **Pairwise and non-pairwise interactions synergize to optimize synchronization.** **a** U-shaped curves are observed for  $\lambda_2(\alpha)$  corresponding to random hypergraphs over a wide range of  $p$  values. **b** Degree-based bound  $|\lambda_2| \leq \frac{n}{n-1}k_{\min}$  predicts the non-monotonic dependence on  $\alpha$ . Each data point represents a 100-node random hypergraph and the three-body connection probability is set to  $p_\Delta = 0.05$ .

tures. In Supplementary Figs. S4 and S5, we show similar results for simplicial complexes constructed from more structured networks, including small-world and scale-free networks.

## B. Linking higher-order representation, degree heterogeneity, and synchronization performance

To gain analytical insight on synchronization stability, we note that the extreme values of the spectrum of a Laplacian can be related to the extreme values of the degrees of the associated graph:  $\lambda_n$  can be bounded by the maximum degree  $k_{\max}$  from both directions,  $\frac{n}{n-1}k_{\max} \leq |\lambda_n| \leq 2k_{\max}$  [66]; and  $\lambda_2$  can be bounded by the minimum degree  $k_{\min}$  from both directions,  $2k_{\min} - n + 2 \leq |\lambda_2| \leq \frac{n}{n-1}k_{\min}$  [67]. For the multiorder Laplacian, the degree  $k_i^{(\text{mul})}$  is given by the weighted sum of degrees of different orders, in this case  $k_i^{(\text{mul})} = \frac{1-\alpha}{\langle k^{(1)} \rangle} k_i^{(1)} + \frac{\alpha}{\langle k^{(2)} \rangle} k_i^{(2)} = L_{ii}^{(\text{mul})}$ . In Fig. 2, we show that  $\frac{n}{n-1}k_{\min}$  is a good approximation for  $|\lambda_2|$  in random hypergraphs and is able to explain the U-shape observed for  $\lambda_2(\alpha)$ .

These degree-based bounds allow us to understand the opposite dependence on  $\alpha$  for random hypergraphs and simplicial complexes. For simplicial complexes, the reason for the deterioration of synchronization stability is the following: Adding 2-simplices to triangles makes the network more heterogeneous (degree-rich nodes get richer; well-connected parts of the network become even more highly connected), thus making the Laplacian eigenvalues (and Lyapunov exponents) more spread out.

To quantify this rich-get-richer effect, we focus on simplicial complexes constructed from Erdős–Rényi graphs  $G(n, p)$ . In this case, we can derive the relationship be-

tween the first-order degrees  $k^{(1)}$  and second-order degrees  $k^{(2)}$  (below we suppress the subscript  $i$  to ease the notation when possible). If node  $i$  has first-order degree  $k^{(1)}$ , then there are at most  $\binom{k^{(1)}}{2}$  2-simplices that can potentially be attached to it. For example, when node  $i$  is connected to nodes  $j$  and  $k$ , then the 2-simplex  $\Delta_{ijk}$  is present if and only if node  $j$  is also connected to node  $k$ . Because the edges are independent in  $G(n, p)$ , when the network is not too sparse, we should expect about  $p\binom{k^{(1)}}{2}$  2-simplices attached to node  $i$ :

$$k^{(2)} \approx \mathbb{E}[k^{(2)}] = p \binom{k^{(1)}}{2} = pk^{(1)}(k^{(1)} - 1)/2. \quad (6)$$

This quadratic dependence of  $k^{(2)}$  on  $k^{(1)}$  provides a foundation for the rich-get-richer effect. To further quantify how the degree heterogeneity changes going from the first-order interaction to the second-order interaction, we calculate the following heterogeneity ratio

$$r = \frac{k_{\max}^{(2)}/k_{\min}^{(2)}}{k_{\max}^{(1)}/k_{\min}^{(1)}}. \quad (7)$$

If  $r > 1$ , it means there is higher degree heterogeneity among 2-simplices than in the pairwise network, which translates into worse synchronization stability in the presence of higher-order interactions. Plugging Eq. (6) into Eq. (7), we obtain

$$r \approx k_{\max}^{(1)}/k_{\min}^{(1)} \geq 1. \quad (8)$$

This shows that the coupling structure of 2-simplices is always more heterogeneous than 1-simplices for simplicial complexes constructed from Erdős–Rényi graphs. Moreover, the more heterogeneous is the pairwise network, the bigger the difference between first-order and second-order couplings in terms of heterogeneity. Specifically, because Erdős–Rényi graphs are more heterogeneous for smaller  $p$ , the heterogeneity ratio  $r$  becomes larger for smaller  $p$ .

Figure 3a shows  $k^{(1)}$  vs.  $k^{(2)}$  for three simplicial complexes with  $n = 300$  and various values of  $p$ . The relationship between  $k^{(1)}$  and  $k^{(2)}$  is well predicted by Eq. (6). The heterogeneity ratio  $r$  is marked beside each data set and closely follows Eq. (8). Figure 3b shows  $r$  as a function of  $p$  for  $n = 300$ . The error bar represents the standard deviation estimated from 1000 samples. The data confirm our prediction that  $r > 1$  for all considered simplicial complexes, and the difference between the first-order and second-order degree heterogeneities is most pronounced when the pairwise connections are sparse.

Next, we turn to the case of random hypergraphs and explain why higher-order interactions promote synchronization in this case (assuming that  $p = p_{\Delta}$ ). For Erdős–Rényi graphs  $G(n, p)$ , the degree of each node is a random variable drawn from the binomial distribution  $B(k; n, p) = \binom{n}{k} p^k q^{n-k}$ , where  $\binom{n}{k}$  is the binomial coefficient and  $q = 1 - p$ . There are some correlations among the degrees, because if an edge connects nodes  $i$

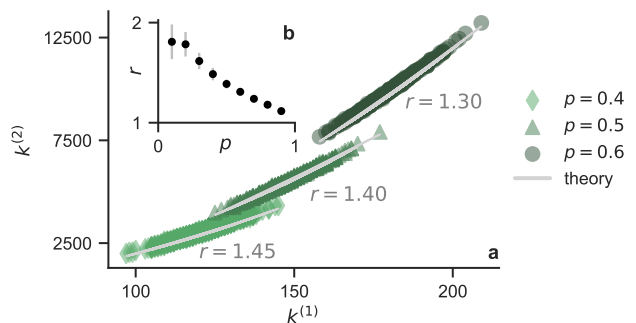


FIG. 3. **Higher-order interactions increase degree heterogeneity in simplicial complexes.** **a** First-order degrees  $k^{(1)}$  and second-order degrees  $k^{(2)}$  follow Eq. (6) for simplicial complexes constructed from Erdős–Rényi graphs. The heterogeneity ratio  $r$  is well approximated by Eq. (8). **b** Degree heterogeneity of the three-body couplings is larger than that of the pairwise couplings in simplicial complexes for all values of  $p$  (i.e.,  $r$  is always greater than 1).

and  $j$ , then it adds to the degree of both nodes. However, the induced correlations are weak and the degrees can almost be treated as independent random variables for sufficiently large  $n$  (the degrees would be truly independent if the Erdős–Rényi graphs were directed). The distribution of the maximum degree for large  $n$  is given in Ref. [68]:

$$P\left(k_{\max}^{(1)} < pn + (2pqn \log n)^{1/2} f(n, y)\right) \approx e^{-e^{-y}}, \quad (9)$$

where  $f(n, y) = 1 - \frac{\log \log n}{4 \log n} - \frac{\log(\sqrt{2\pi})}{2 \log n} + \frac{y}{2 \log n}$ .

For generalized degrees  $k^{(2)}$ , the degree correlation induced by three-body couplings is stronger than the case of pairwise interactions, but it is still a weak correlation for large  $n$ . To estimate the expected value of the maximum degree, one needs to solve the following problem from order statistics: Given a binomial distribution and  $n$  independent random variables  $k_i$  drawn from it, what is the expected value of the largest random variable  $\mathbb{E}[k_{\max}]$ ? Denoting the cumulative distribution of  $B(N, p)$  as  $F(N, p)$ , where  $N = (n-1)(n-2)/2$  is the number of possible 2-simplices attached to a node, the cumulative distribution of  $k_{\max}^{(2)}$  is simply given by  $F(N, p)^n$ . However, because  $F(N, p)$  does not have a closed-form expression, it is not easy to extract useful information from the result above.

To gain analytical insights, we turn to Eq. (9) with  $n$  replaced by  $N$ , which serves as an upper bound for the distribution of  $k_{\max}^{(2)}$ . To see why, notice that Eq. (9) gives the distribution of  $k_{\max}^{(1)}$  for  $n$  (weakly-correlated) random variables  $k_i^{(1)}$  drawn from  $B(n, p)$ . For  $k_{\max}^{(2)}$ , we are looking at  $n$  random variables  $k_i^{(2)}$  with slightly stronger correlations than  $k_i^{(1)}$ , now drawn from  $B(N, p)$ . Thus, Eq. (9) with  $n$  replaced by  $N$  gives the distribution of  $k_{\max}^{(2)}$  if one had more samples ( $N$  instead of  $n$ ) and weaker correlations. Both factors lead to an overes-



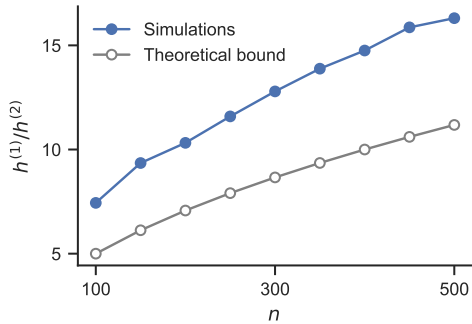


FIG. 4. **Higher-order interactions decrease degree heterogeneity in random hypergraphs.** The degree heterogeneity (measured by  $h^{(1)}$  and  $h^{(2)}$ ) is stronger in the first-order Laplacian  $\mathbf{L}^{(1)}$  than in the second-order Laplacian  $\mathbf{L}^{(2)}$ , and the difference increases with system size  $n$ . The theoretical lower bound of  $\frac{h^{(1)}}{h^{(2)}}$  is given by  $\frac{\sqrt{n}}{2}$  and is independent of  $p$ . The simulation results are obtained from random hypergraphs with different sizes  $n$ , using 500 samples for each  $n$ . The connection probabilities are set to  $p = p_{\Delta} = 0.1$ .

timization of  $\mathbb{E}[k_{\max}^{(2)}]$ , but their effects are expected to be small.

To summarize, we have

$$P\left(k_{\max}^{(2)} < pN + (2pqN \log N)^{1/2} f(N, y)\right) > e^{-e^{-y}}. \quad (10)$$

Solving  $e^{-e^{-y_0}} = \frac{1}{2}$  gives  $y_0 \approx 0.52$ . Plugging  $y_0$  into the left hand side of Eqs. (9) and (10) yields an estimate of the expected values of  $k_{\max}^{(1)}$  and  $k_{\max}^{(2)}$ , respectively. (Note that here for simplicity, we use the median to approximate the expected value.) Through symmetry, one can also easily obtain the expected values of  $k_{\min}^{(1)}$  and  $k_{\min}^{(2)}$ . To measure the degree heterogeneity, we can compute the heterogeneity indexes

$$h^{(1)} = (\mathbb{E}[k_{\max}^{(1)}] - \mathbb{E}[\overline{k^{(1)}}]) / \mathbb{E}[\overline{k^{(1)}}], \quad (11)$$

$$h^{(2)} = (\mathbb{E}[k_{\max}^{(2)}] - \mathbb{E}[\overline{k^{(2)}}]) / \mathbb{E}[\overline{k^{(2)}}], \quad (12)$$

which controls  $\lambda_2$  through degree-based bounds. Here, the expected values of the mean degree are given by  $\mathbb{E}[\overline{k^{(1)}}] = pn$  and  $\mathbb{E}[\overline{k^{(2)}}] = pN$ , respectively.

Now, how do the first-order and second-order degree heterogeneities compare against each other? Using Eqs. (9), (10) and (12), we see that

$$\frac{h^{(1)}}{h^{(2)}} > \frac{(2qn^{-1} \log n)^{1/2} f(n, y_0)}{(2qN^{-1} \log N)^{1/2} f(N, y_0)}. \quad (13)$$

For large  $n$ , we can assume  $f(n, y_0) \approx f(N, y_0) \approx 1$  and simplify Eq. (13) into

$$\frac{h^{(1)}}{h^{(2)}} > \frac{(n^{-1} \log n)^{1/2}}{(N^{-1} \log N)^{1/2}} \approx \frac{\sqrt{n}}{2}. \quad (14)$$

First, note that  $\frac{h^{(1)}}{h^{(2)}} > 1$  for almost all  $n$ , which translates into better synchronization stability in the presence of

higher-order interactions. The scaling also tells us that, as  $n$  is increased, the difference in degree heterogeneities becomes more pronounced. The theoretical lower bound [Eq. (14)] is compared to simulation results in Fig. 4, which show good agreement. Intuitively, the (normalized) second-order Laplacian has a much narrower spectrum compared to the first-order Laplacian with the same  $p$  because binomial distributions are more concentrated for larger  $n$  (i.e., there is much less relative fluctuation around the mean degree for  $k^{(2)}$  compared to  $k^{(1)}$ ).

### C. Exploring the hypergraph space with synthetic networks and brain networks

So far we have focused mostly on simplicial complexes and random hypergraphs, which offered analytical insights into how higher-order representations influence collective dynamics. However, a vast portion of the hypergraph space is occupied by hypergraphs that are not simplicial complexes or random hypergraphs. What is the effect of higher-order interactions there? To explore the hypergraph space more thoroughly, we first construct simplicial complexes from both synthetic networks and real brain networks. We then study the synchronization stability of these structures as they move further and further away from being a simplicial complex. We find that as the distance to being a simplicial complex is increased, higher-order interactions quickly switch from impeding synchronization to promoting synchronization. This echoes the analytical results obtained above for simplicial complexes and random hypergraphs, and it supports our conclusion that higher-order interactions enhance synchronization in a broad class of (both structured and random) hypergraphs, except when they are close to being a simplicial complex.

Specifically, we consider the animal connectome data from Neurodata.io [69], which consists of neuronal networks from different brain regions and different animal species. We chose brain networks because it has been shown that nonpairwise interactions and synchronization dynamics are both important in the brain [5, 70]. For the sake of computational efficiency, we selected six networks spanning three different species (worm, monkey, and cat) that are neither too dense nor too sparse. Specifically, for each brain network, we first construct a simplicial complex by filling all 3-cliques (i.e., closed triangles) with 2-simplices. In reality, not all 3-cliques imply the existence of three-body interactions, and not all three-body interactions reside within 3-cliques. Thus, we continue by shuffling each 2-simplex to a random location in the hypergraph with probability  $p_s$ . This allows us to explore hypergraph structures beyond simplicial complexes and random hypergraphs, with  $p_s$  also serving as a proxy for the distance between the hypergraph structure and the original simplicial complex.

Figure 5 shows the synchronization stability  $\lambda_2(\alpha)$  for hypergraphs constructed from the six brain networks

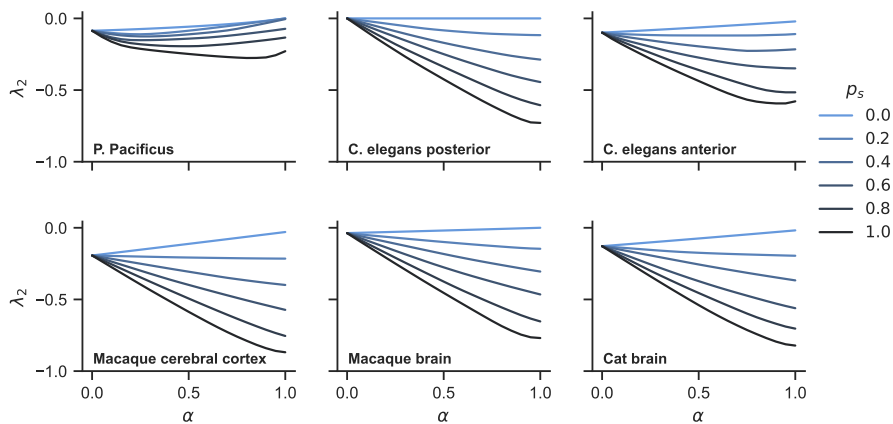


FIG. 5. **Synchronization stability of hypergraphs constructed from brain networks.** For each of the six brain networks, we start by attaching 2-simplices to closed triangles and turning the network into a simplicial complex. We then construct hypergraphs at different distances from the simplicial complex by randomly shuffling the 2-simplices with probability  $p_s$ . For each value of  $p_s$ , we plot synchronization stability  $\lambda_2$  as a function of the control parameter  $\alpha$  (averaged over 50 independent realizations). It is clear that as the hypergraphs move further away from being a simplicial complex, synchronization stability is consistently improved. The role of higher-order interactions also generally transitions from impeding synchronization to promoting synchronization as  $p_s$  is increased.

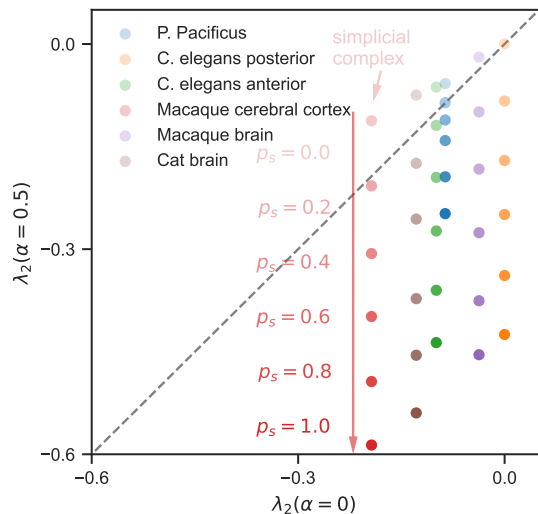


FIG. 6. **Nonpairwise interactions typically enhance synchronization in hypergraphs, except when they are close to being a simplicial complex.** This plot uses the same data as in Fig. 5 and explicitly shows the transition in how higher-order interactions affect synchronization as the hypergraph structure loses resemblance to simplicial complexes. Points in the upper-left half of the square represent hypergraphs for which higher-order interactions impede synchronization, while points in the lower-right half of the square represent hypergraphs for which higher-order interactions promote synchronization. As the shuffling probability  $p_s$  is increased ( $p_s = 0$  corresponds to simplicial complexes), all six systems swiftly move across the diagonal line and into the synchronization-promoting region.

at different values of shuffling probability  $p_s$ . Here, each curve represents an average  $\lambda_2(\alpha)$  over 100 independent realizations of the hypergraph structure at a given  $p_s$ . We see that as  $p_s$  is increased, for all sys-

tems, the curves change from going upward (or staying level for the disconnected *C. elegans* posterior network) with  $\alpha$  to going downward with  $\alpha$ , signaling a transition from hyperedge-impeded synchronization to hyperedge-enhanced synchronization. Thus, the opposite trends we observed for simplicial complexes and random hypergraphs remain valid for a broad class of hypergraphs constructed from real-world networks.

Figure 6 summarizes the same result from a different perspective by plotting  $\lambda_2(\alpha = 0.5)$  against  $\lambda_2(\alpha = 0)$  at different values of  $p_s$  (other choices of the two  $\alpha$  values give similar results). As  $p_s$  is increased from 0 to 1 and the hypergraph structure moves further away from being a simplicial complex, we see all six systems transition from the upper-left half of the plot (higher-order interactions impeding synchronization) to the lower-right half of the plot (higher-order interactions promoting synchronization). Moreover, the transitions happen fairly rapidly, with all systems crossing the diagonal line at  $p_s < 0.2$ .

We also find similar results for hypergraphs constructed from synthetic networks including scale-free and small-world networks, which we show in Supplementary Figs. S6 and S7, and for real-world hypergraphs (Supplementary Fig. S8). One additional thing worth noting in Supplementary Figs. S6 and S7 is that as long as the network is not too sparse or dense, changing the network density mostly shifts all curves together in the vertical direction without affecting the transition from hyperedge-impeded synchronization to hyperedge-enhanced synchronization.

#### D. The role of degree correlation

Cross-order degree correlation, defined as the correlation between the degree vectors at each order,  $DC = \text{corr}(\{k_i^{(1)}\}, \{k_i^{(2)}\})$ , has been shown to affect epidemic spreading and synchronization, where it can promote the onset of bistability and hysteresis [71, 72]. By construction, degree correlation is large and positive in simplicial complexes due to the inclusion condition and close to zero in random hypergraphs. Here, we investigate the effect of cross-order degree correlation on synchronization to provide a more complete picture on why higher-order representations matter.

To isolate the effects of degree correlation from those of degree heterogeneity, we propose a method to fix the latter while changing the former. Starting from a simplicial complex, we first select two nodes: a node  $i$  included in only a few triangles (low  $k_i^{(2)}$ ) and a node  $j$  included in many triangles (large  $k_j^{(2)}$ ). Then we swap their respective values of  $k^{(2)}$  by swapping the 2-simplices node  $i$  and node  $j$  belong to. The hyperedge membership swap has the expected effect: it lowers the degree correlation without changing the degree heterogeneity. How much the swap lowers the correlation depends on the respective degrees of the nodes at each order. In particular, a simple way to maximize this effect is to iteratively swap the nodes that have the lowest and the largest  $k^{(2)}$ . Note that this swapping procedure is different from the shuffling procedure used for Figs. 5 and 6 (shuffling does not preserve the second-order degree sequence).

In Fig. 7, we show the result of the hyperedge membership swap on the cat brain network. The starting simplicial complex is the one used in Fig. 5, for which we do not swap any memberships. Then, we build two hypergraphs from it by selecting 5 and 15 pairs of nodes and swapping their 2-simplices as described above. As a result,  $\lambda_2$  is lowered for intermediate values of  $\alpha$ . Importantly, though, the endpoints  $\lambda_2(\alpha = 0)$  and  $\lambda_2(\alpha = 1)$  are left unchanged, since only one order of interactions are present. These observations are confirmed on hypergraphs constructed from the other five brain networks (Supplementary Fig. S9) and from synthetic networks (Supplementary Fig. S10).

To summarize, lowering the cross-order degree correlation can help improve the synchronization stability when there is a mixture of pairwise and nonpairwise interactions. Intuitively, this makes sense because negative correlation allows the degree heterogeneity from two different orders of interactions to compensate each other and homogenize the hypergraph structure.

### III. DISCUSSION

To conclude, using simple phase oscillators, we have shown that higher-order interactions promote synchronization in a broad class of hypergraphs but impede it

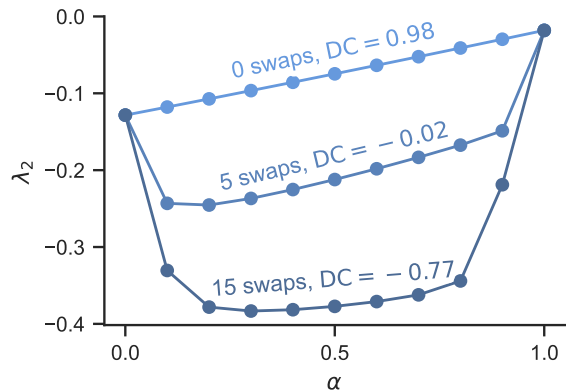


FIG. 7. **Cross-order degree correlation affects synchronization stability in systems with mixed pairwise and nonpairwise interactions ( $0 < \alpha < 1$ ), but not in the uniform cases ( $\alpha = 0$  and  $\alpha = 1$ ).** The hypergraphs are constructed from the cat brain dataset. For each curve, we indicate the number of pairs of nodes selected for the hyperedge membership swapping procedure (see text for details). The procedure changes the cross-order degree correlation (DC) without affecting the degree sequences (thus also the degree heterogeneity ratio). We can see that more negative cross-order degree correlation translates into better synchronization stability.

in simplicial complexes. We identify higher-order degree heterogeneity and degree correlation as the underlying mechanism driving the opposite trends. While we only considered two-body and three-body couplings, the same framework naturally extends to the case of larger group interactions.

Do the lessons obtained here for phase oscillators carry over to more general oscillator dynamics? The generalized Laplacians used here have been shown to work for arbitrary oscillator dynamics and coupling functions [41]. Similarly, the spread of eigenvalues of each Laplacian carries critical information on the synchronizability of the corresponding level of interactions. Thus, once different orders of coupling functions have been properly normalized, we expect the findings here to transfer to systems beyond coupled phase oscillators. That is, for generic oscillator dynamics, higher-order interactions should in general promote synchronization if the hyperedges are more uniformly distributed than their pairwise counterpart. In the future, it would be interesting to generalize our results to systems whose interactions can be nonreciprocal [73–76].

Finally, while here we focused on the synchronization of coupled oscillators, our results are likely to have implications for other processes. These include dynamics as different as diffusion [30], contagion [71], and evolutionary processes [36], in which degree heterogeneity and degree correlation play a key role, and yet the differences between simplicial complexes and hypergraphs have been mostly treated as inconsequential. All in all, our results suggest that simplicial complexes and hypergraphs cannot always be used interchangeably and future

works should consider the influence of the chosen representation when interpreting their results.

**Data availability:** The brain connectome data used in Figs. 5 to 7 can be found at <https://neurodata.io/project/connectomes/>. All other data needed to evaluate our results are present in the paper. Additional data related to this paper may be requested from the authors.

**Code availability:** The code to reproduce the main results is available at [https://github.com/maximelucas/HOI\\_shape\\_sync\\_differently](https://github.com/maximelucas/HOI_shape_sync_differently) or on Zenodo <https://doi.org/10.5281/zenodo.7662113> [77], and makes use

of the XGI library [78].

**Acknowledgements:** We thank Alessio Lapolla, George Cantwell, Giovanni Petri, Nicholas Landry, and Steven Strogatz for insightful discussions. Y.Z. acknowledges support from the Schmidt Science Fellowship and Omidyar Fellowship. M.L. acknowledges partial support from Intesa Sanpaolo Innovation Center.

**Author Contributions:** Y.Z., M.L., and F.B. conceived the research. Y.Z. and M.L. performed the research. Y.Z., M.L., and F.B. wrote the manuscript.

**Competing Interests:** The authors declare that they have no competing interests.

- 
- [1] S. Boccaletti, V. Latora, Y. Moreno, M. Chavez, and D.-U. Hwang, Complex networks : Structure and dynamics, *Phys. Rep.* **424**, 175 (2006).
- [2] M. E. J. Newman, *Networks: An Introduction* (Oxford University Press, 2010).
- [3] R. Lambiotte, M. Rosvall, and I. Scholtes, From networks to optimal higher-order models of complex systems, *Nat. Phys.* **15**, 313 (2019).
- [4] F. Battiston, G. Cencetti, I. Iacopini, V. Latora, M. Lucas, A. Patania, J.-G. Young, and G. Petri, Networks beyond pairwise interactions: Structure and dynamics, *Phys. Rep.* **874**, 1 (2020).
- [5] L. Torres, A. S. Blevins, D. Bassett, and T. Eliassi-Rad, The Why, How, and When of Representations for Complex Systems, *SIAM Rev.* **63**, 435 (2021).
- [6] F. Battiston, E. Amico, A. Barrat, G. Bianconi, G. Ferraz de Arruda, B. Franceschiello, I. Iacopini, S. Kéfi, V. Latora, Y. Moreno, M. M. Murray, T. P. Peixoto, F. Vaccarino, and G. Petri, The physics of higher-order interactions in complex systems, *Nat. Phys.* **17**, 1093 (2021).
- [7] F. Battiston and G. Petri, *Higher-Order Systems* (Springer, 2022).
- [8] G. Cencetti, F. Battiston, B. Lepri, and M. Karsai, Temporal properties of higher-order interactions in social networks, *Sci. Rep.* **11**, 7028 (2021).
- [9] A. Patania, G. Petri, and F. Vaccarino, The shape of collaborations, *EPJ Data Sci.* **6**, 18 (2017).
- [10] J. Grilli, G. Barabás, M. J. Michalska-Smith, and S. Allesina, Higher-order interactions stabilize dynamics in competitive network models, *Nature* **548**, 210 (2017).
- [11] G. Petri, P. Expert, F. Turkheimer, R. Carhart-Harris, D. Nutt, P. J. Hellyer, and F. Vaccarino, Homological scaffolds of brain functional networks, *J R Soc Interface* **11**, 20140873 (2014).
- [12] C. Giusti, R. Ghrist, and D. S. Bassett, Two’s company, three (or more) is a simplex, *J. Comput. Neurosci.* **41**, 1 (2016).
- [13] E. Estrada and J. A. Rodríguez-Velázquez, Subgraph centrality and clustering in complex hyper-networks, *Phys. A* **364**, 581 (2006).
- [14] A. R. Benson, R. Abebe, M. T. Schaub, A. Jadbabaie, and J. Kleinberg, Simplicial closure and higher-order link prediction, *Proc. Natl. Acad. Sci. U.S.A* **115**, E11221 (2018).
- [15] A. R. Benson, Three hypergraph eigenvector centralities, *SIAM J. Math. Data Sci.* **1**, 293 (2019).
- [16] F. Musciotto, F. Battiston, and R. N. Mantegna, Detecting informative higher-order interactions in statistically validated hypergraphs, *Commun. Phys.* **4**, 218 (2021).
- [17] T. Carletti, D. Fanelli, and R. Lambiotte, Random walks and community detection in hypergraphs, *J. Phys. Complex* **2**, 015011 (2021).
- [18] A. Eriksson, D. Edler, A. Rojas, M. de Domenico, and M. Rosvall, How choosing random-walk model and network representation matters for flow-based community detection in hypergraphs, *Commun. Phys.* **4**, 133 (2021).
- [19] P. S. Chodrow, N. Veldt, and A. R. Benson, Generative hypergraph clustering: From blockmodels to modularity, *Sci. Adv.* **7**, eabh1303 (2021).
- [20] M. Contisciani, F. Battiston, and C. De Bacco, Inference of hyperedges and overlapping communities in hypergraphs, *Nat. Commun.* **13**, 7229 (2022).
- [21] Q. F. Lotito, F. Musciotto, A. Montresor, and F. Battiston, Higher-order motif analysis in hypergraphs, *Commun. Phys.* **5**, 79 (2022).
- [22] C. Bick, P. Ashwin, and A. Rodrigues, Chaos in generically coupled phase oscillator networks with nonpairwise interactions, *Chaos* **26**, 094814 (2016).
- [23] C. Bick, Heteroclinic dynamics of localized frequency synchrony: Heteroclinic cycles for small populations, *J. Nonlin. Sci.* **29**, 2571 (2019).
- [24] P. S. Skardal and A. Arenas, Abrupt desynchronization and extensive multistability in globally coupled oscillator simplexes, *Phys. Rev. Lett.* **122**, 248301 (2019).
- [25] P. S. Skardal and A. Arenas, Higher order interactions in complex networks of phase oscillators promote abrupt synchronization switching, *Commun. Phys.* **3**, 218 (2020).
- [26] C. Xu, X. Wang, and P. S. Skardal, Bifurcation analysis and structural stability of simplicial oscillator populations, *Phys. Rev. Res.* **2**, 023281 (2020).
- [27] Y. Zhang, V. Latora, and A. E. Motter, Unified treatment of synchronization patterns in generalized networks with higher-order, multilayer, and temporal interactions, *Commun. Phys.* **4**, 195 (2021).
- [28] C. Kuehn and C. Bick, A universal route to explosive phenomena, *Sci. Adv.* **7**, eabe3824 (2021).
- [29] M. T. Schaub and S. Segarra, Flow smoothing and denoising: Graph signal processing in the edge-space, in *2018 IEEE Global Conference on Signal and Information Processing (GlobalSIP)* (IEEE, 2018) pp. 735–739.
- [30] T. Carletti, F. Battiston, G. Cencetti, and D. Fanelli,



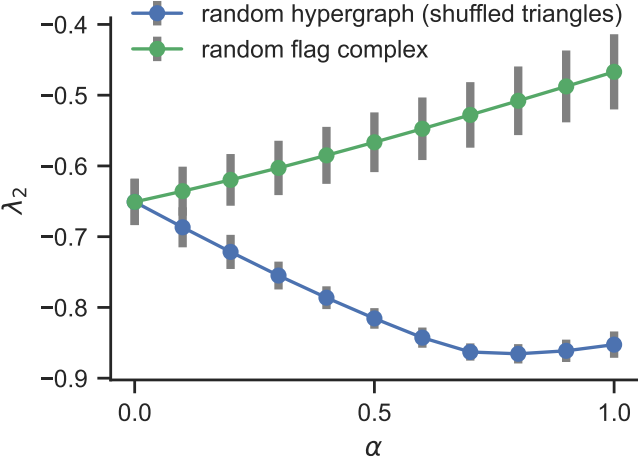
- Random walks on hypergraphs, *Phys. Rev. E* **101**, 022308 (2020).
- [31] L. Neuhäuser, A. Mellor, and R. Lambiotte, Multibody interactions and nonlinear consensus dynamics on networked systems, *Phys. Rev. E* **101**, 032310 (2020).
- [32] L. DeVille, Consensus on simplicial complexes: Results on stability and synchronization, *Chaos* **31**, 023137 (2021).
- [33] I. Iacopini, G. Petri, A. Barrat, and V. Latora, Simplicial models of social contagion, *Nat. Commun.* **10**, 2485 (2019).
- [34] G. Ferraz de Arruda, M. Tizzani, and Y. Moreno, Phase transitions and stability of dynamical processes on hypergraphs, *Commun. Phys.* **4**, 24 (2021).
- [35] S. Chowdhary, A. Kumar, G. Cencetti, I. Iacopini, and F. Battiston, Simplicial contagion in temporal higher-order networks, *J. Phys. Complex* **2**, 035019 (2021).
- [36] U. Alvarez-Rodriguez, F. Battiston, G. F. de Arruda, Y. Moreno, M. Perc, and V. Latora, Evolutionary dynamics of higher-order interactions in social networks, *Nat. Hum. Behav* **5**, 586 (2021).
- [37] C. C. Gong and A. Pikovsky, Low-dimensional dynamics for higher-order harmonic, globally coupled phase-oscillator ensembles, *Phys. Rev. E* **100**, 062210 (2019).
- [38] A. P. Millán, J. J. Torres, and G. Bianconi, Explosive Higher-Order Kuramoto Dynamics on Simplicial Complexes, *Phys. Rev. Lett.* **124**, 218301 (2020).
- [39] M. Lucas, G. Cencetti, and F. Battiston, Multiorder Laplacian for synchronization in higher-order networks, *Phys. Rev. Res.* **2**, 033410 (2020).
- [40] A. Arnaudon, R. L. Peach, G. Petri, and P. Expert, Connecting hodge and sakaguchi-kuramoto through a mathematical framework for coupled oscillators on simplicial complexes, *Commun. Phys.* **5**, 211 (2022).
- [41] L. V. Gambuzza, F. Di Patti, L. Gallo, S. Lepri, M. Romance, R. Criado, M. Frasca, V. Latora, and S. Boccaletti, Stability of synchronization in simplicial complexes, *Nat. Commun.* **12**, 1255 (2021).
- [42] A. Salova and R. M. D'Souza, Cluster synchronization on hypergraphs, arXiv:2101.05464 (2021).
- [43] F. Baccini, F. Geraci, and G. Bianconi, Weighted simplicial complexes and their representation power of higher-order network data and topology, *Phys. Rev. E* **106**, 034319 (2022).
- [44] C. Berge, *Hypergraphs: Combinatorics of Finite Sets* (Elsevier, 1984).
- [45] A. Hatcher, *Algebraic Topology* (Cambridge University Press, 2002).
- [46] A. Patania, F. Vaccarino, and G. Petri, Topological analysis of data, *EPJ Data Sci.* **6**, 7 (2017).
- [47] M. T. Schaub, A. R. Benson, P. Horn, G. Lippner, and A. Jadbabaie, Random walks on simplicial complexes and the normalized Hodge 1-Laplacian, *SIAM Rev.* **62**, 353 (2020).
- [48] J.-G. Young, G. Petri, and T. P. Peixoto, Hypergraph reconstruction from network data, *Commun. Phys.* **4**, 135 (2021).
- [49] A. Pikovsky, M. Rosenblum, and J. Kurths, *Synchronization: A Universal Concept in Nonlinear Sciences* (Cambridge University Press, 2003).
- [50] A. Arenas, A. Díaz-Guilera, J. Kurths, Y. Moreno, and C. Zhou, Synchronization in complex networks, *Phys. Rep.* **469**, 93 (2008).
- [51] J.-C. Leloup and A. Goldbeter, Toward a detailed computational model for the mammalian circadian clock, *Proc. Natl. Acad. Sci. U.S.A.* **100**, 7051 (2003).
- [52] M. Bračič Lotrič and A. Stefanovska, Synchronization and modulation in the human cardiorespiratory system, *Phys. A* **283**, 451 (2000).
- [53] D. Cumin and C. P. Unsworth, Generalising the Kuramoto model for the study of neuronal synchronisation in the brain, *Phys. D* **226**, 181 (2007).
- [54] P. Ashwin and A. Rodrigues, Hopf normal form with  $S_N$  symmetry and reduction to systems of nonlinearly coupled phase oscillators, *Phys. D* **325**, 14 (2016).
- [55] I. León and D. Pazó, Phase reduction beyond the first order: The case of the mean-field complex Ginzburg-Landau equation, *Phys. Rev. E* **100**, 012211 (2019).
- [56] M. H. Matheny, J. Emenheiser, W. Fon, A. Chapman, A. Salova, M. Rohden, J. Li, M. Hudoba de Badyń, M. Pósfai, L. Duenas-Osorio, *et al.*, Exotic states in a simple network of nanoelectromechanical oscillators, *Science* **363**, eaav7932 (2019).
- [57] E. Gengel, E. Teichmann, M. Rosenblum, and A. Pikovsky, High-order phase reduction for coupled oscillators, *J. Phys. Complex* **2**, 015005 (2020).
- [58] E. Nijholt, J. L. Ocampo-Espindola, D. Eroglu, I. Z. Kiss, and T. Pereira, Emergent hypernetworks in weakly coupled oscillators, *Nat. Commun.* **13**, 4849 (2022).
- [59] P. S. Skardal, L. Arola-Fernández, D. Taylor, and A. Arenas, Higher-order interactions can better optimize network synchronization, *Phys. Rev. Res.* **3**, 043193 (2021).
- [60] K. Kovalenko, X. Dai, K. Alfaro-Bittner, A. M. Raigorodskii, M. Perc, and S. Boccaletti, Contrarians Synchronize beyond the Limit of Pairwise Interactions, *Phys. Rev. Lett.* **127**, 258301 (2021).
- [61] F. Parastesh, M. Mehrabbeik, K. Rajagopal, S. Jafari, and M. Perc, Synchronization in Hindmarsh-Rose neurons subject to higher-order interactions, *Chaos* **32**, 013125 (2022).
- [62] Y. Kuramoto, *Chemical Oscillations, Waves, and Turbulence* (Springer-Verlag, 1984).
- [63] Y. Zhang and S. H. Strogatz, Designing temporal networks that synchronize under resource constraints, *Nat. Commun.* **12**, 3273 (2021).
- [64] M. Dewar, J. Healy, X. Pérez-Giménez, P. Prałat, J. Proos, B. Reiniger, and K. Ternovsky, Subhypergraphs in non-uniform random hypergraphs, arXiv:1703.07686 (2018).
- [65] D. J. Watts and S. H. Strogatz, Collective dynamics of 'small-world' networks, *Nature* **393**, 440 (1998).
- [66] X.-D. Zhang, The Laplacian eigenvalues of graphs: A survey, arXiv:1111.2897 (2011).
- [67] N. M. M. de Abreu, Old and new results on algebraic connectivity of graphs, *Linear Algebra Its Appl.* **423**, 53 (2007).
- [68] B. Bollobás, The distribution of the maximum degree of a random graph, *Discrete Math.* **32**, 201 (1980).
- [69] <https://neurodata.io/project/connectomes/>.
- [70] R. M. Reinhart and J. A. Nguyen, Working memory revived in older adults by synchronizing rhythmic brain circuits, *Nat. Neurosci* **22**, 820 (2019).
- [71] N. W. Landry and J. G. Restrepo, The effect of heterogeneity on hypergraph contagion models, *Chaos* **30**, 103117 (2020).
- [72] S. Adhikari, J. G. Restrepo, and P. S. Skardal, Synchronization of phase oscillators on complex hypergraphs, *Chaos* **33**, 033116 (2023).

- [73] F. M. Brady, Y. Zhang, and A. E. Motter, Forget partitions: Cluster synchronization in directed networks generate hierarchies, [arXiv:2106.13220](https://arxiv.org/abs/2106.13220) (2021).
- [74] M. Fruchart, R. Hanai, P. B. Littlewood, and V. Vitelli, Non-reciprocal phase transitions, *Nature* **592**, 363 (2021).
- [75] Y. Tang, D. Shi, and L. Lü, Optimizing higher-order network topology for synchronization of coupled phase oscillators, *Commun. Phys.* **5**, 96 (2022).
- [76] L. Gallo, R. Muolo, L. V. Gambuzza, V. Latora, M. Frasca, and T. Carletti, Synchronization induced by directed higher-order interactions, *Commun. Phys.* **5**, 263 (2022).
- [77] Y. Zhang\*, M. Lucas\*, and F. Battiston, Higher-order interactions shape collective dynamics differently in hypergraphs and simplicial complexes (code repository: [HOI\\_shape\\_sync\\_differently](https://github.com/HOI_shape_sync_differently)) (2023), v1.0.
- [78] N. Landry, L. Torres, I. Iacopini, M. Lucas, G. Petri, A. Patania, A. Schwarze, and M. Contisciani, *Complex Group Interactions (XGI)*, v0.5.1.

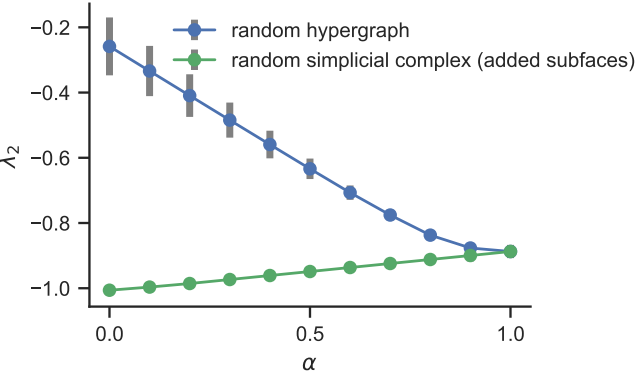
# Supplementary Information

## Higher-order interactions shape collective dynamics differently in hypergraphs and simplicial complexes

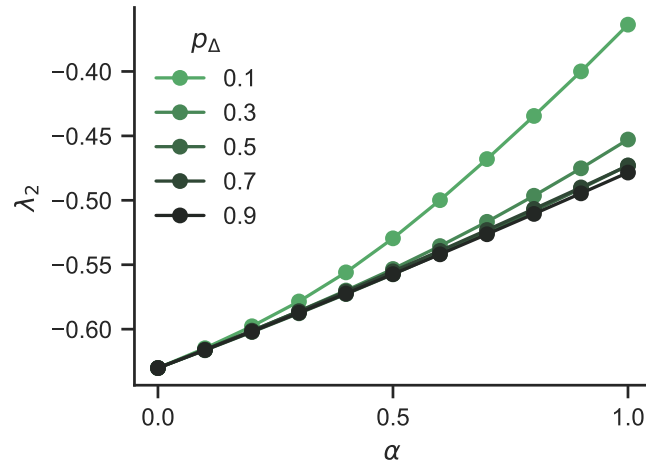
Yuanzhao Zhang, Maxime Lucas, and Federico Battiston



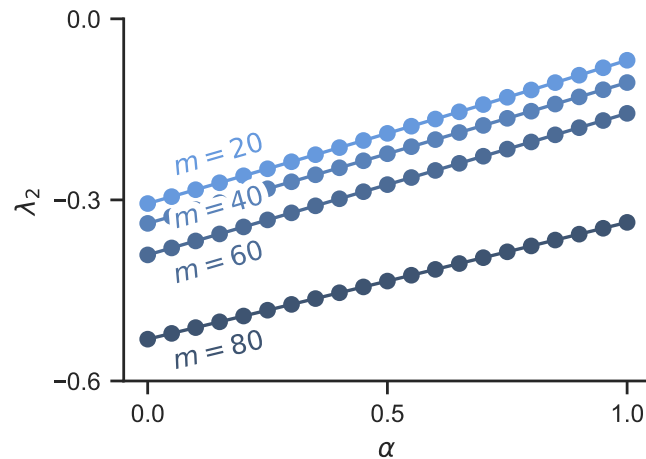
Supplementary Figure S1. **Synchronization is enhanced by higher-order interactions in random hypergraphs but is impeded in simplicial complexes.** Here, we build the simplicial complexes as random flag complexes by generating ER graphs with wiring probability  $p$  and filling all closed triangles with 2-simplices. For each realisation, we build a corresponding random hypergraph by keeping the same 1-hyperedges but move each 2-hyperedge to a random location. This ensures that the random hypergraph has the same number of 1-hyperedges and 2-hyperedges as the original simplicial complex. The maximum transverse Lyapunov exponent  $\lambda_2$  is plotted against  $\alpha$  for random hypergraphs (blue) and simplicial complexes (green). As  $\alpha$  is increased, the coupling goes from first-order-only ( $\alpha = 0$ ) to second-order-only ( $\alpha = 1$ ). Each point represents the average over 5 independent hypergraphs or simplicial complexes with  $n = 100$  nodes. The error bars represent standard deviations. We set  $p = 0.4$  for the simplicial complexes.



Supplementary Figure S2. **Synchronization is enhanced by higher-order interactions in random hypergraphs but is impeded in simplicial complexes.** Here, we build the random hypergraphs by generating each possible 1-hyperedge and 2-hyperedge with probabilities  $p$  and  $p_\Delta$ , respectively. For each realisation, we build a corresponding random simplicial complex by adding 1-hyperedges to satisfy the inclusion condition. The maximum transverse Lyapunov exponent  $\lambda_2$  is plotted against  $\alpha$  for random hypergraphs (blue) and simplicial complexes (green). As  $\alpha$  is increased, the coupling goes from first-order-only ( $\alpha = 0$ ) to second-order-only ( $\alpha = 1$ ). Each point represents the average over 5 independent hypergraphs or simplicial complexes with  $n = 100$  nodes. The error bars represent standard deviations. We set  $p = p_\Delta = 0.1$  for the random hypergraphs.

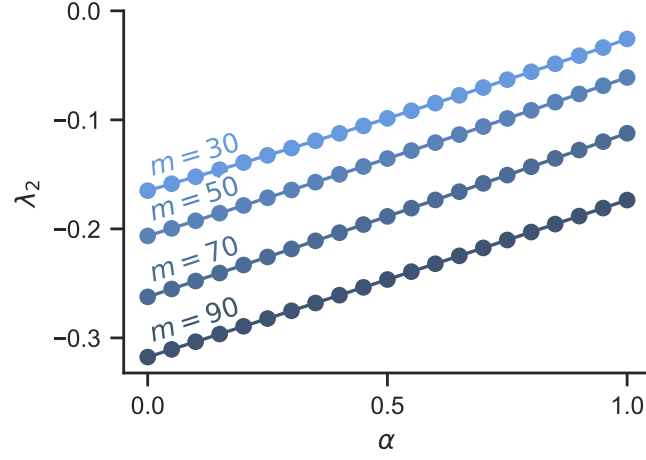


Supplementary Figure S3. **Synchronization is impeded by higher-order interactions in simplicial complexes regardless of the probability of closed triangles being filled.** Here, we build the simplicial complexes as random flag complexes by generating ER graphs with wiring probability  $p$  and filling closed triangles with probability  $p_\Delta$ , for a range of  $p_\Delta$  values. The maximum transverse Lyapunov exponent  $\lambda_2$  is plotted against  $\alpha$ . As  $\alpha$  is increased, the coupling goes from first-order-only ( $\alpha = 0$ ) to second-order-only ( $\alpha = 1$ ). Each point represents the average over 50 independent simplicial complexes with  $n = 100$  nodes. We set  $p = 0.4$  for the generation of the original ER graphs.

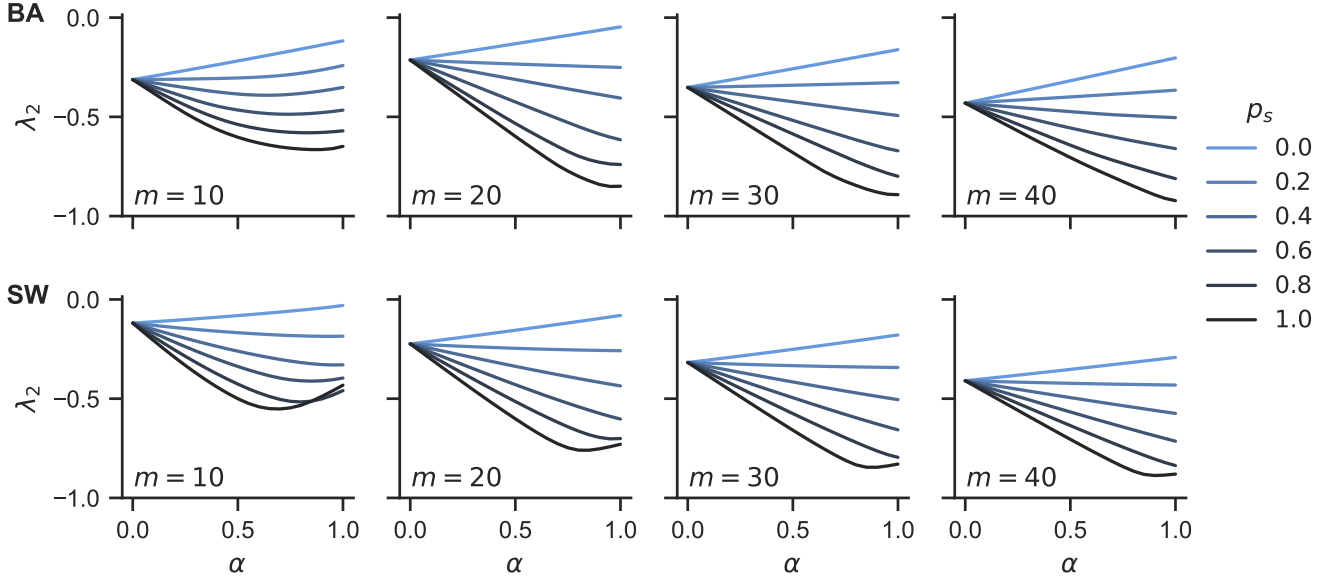


Supplementary Figure S4. **Nonpairwise interactions impede synchronization in simplicial complexes constructed from scale-free networks.** Here, each curve corresponds to a simplicial complex constructed from a scale-free network with  $n = 300$  nodes and mean degree  $2m$ . A scale-free network of  $n$  nodes is grown by starting from an  $m$ -clique and attaching each new node to  $m$  existing nodes. The probability of attachment is proportional to the current degrees of the existing nodes.

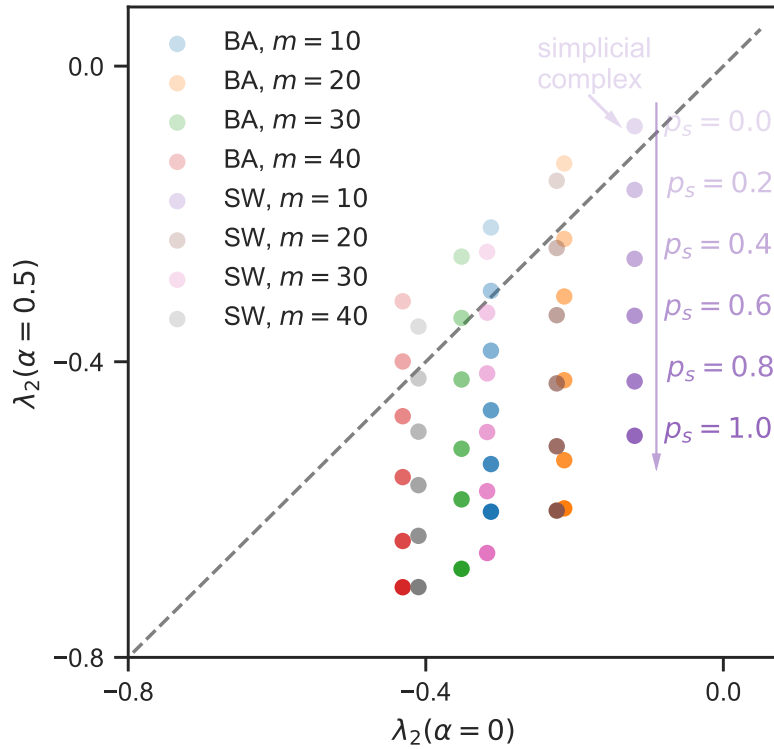




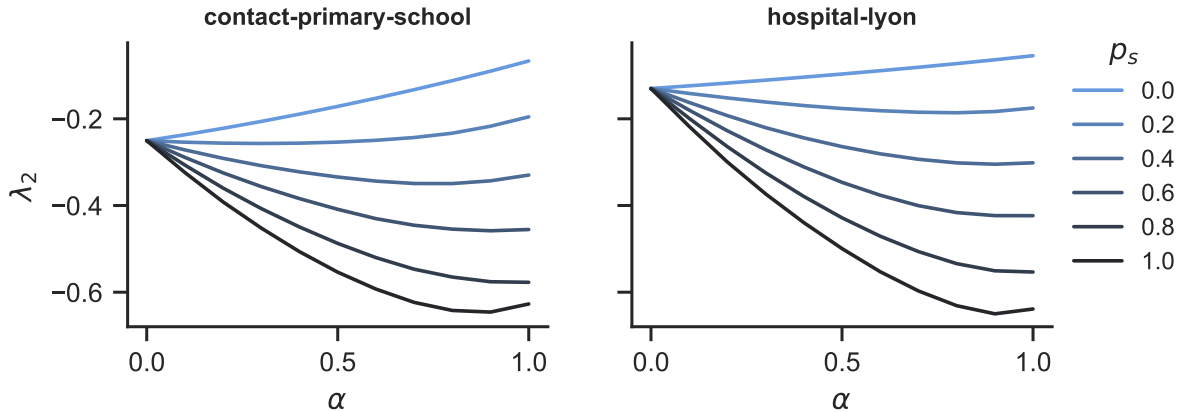
Supplementary Figure S5. **Nonpairwise interactions impede synchronization in simplicial complexes constructed from small-world networks.** Here, each curve corresponds to a simplicial complex constructed from a small-world network with  $n = 300$  nodes and mean degree  $m$ . A small-world network of  $n$  nodes is constructed by starting from a ring network with each node joined with its  $m$  nearest neighbors and randomly rewiring each link with probability  $p_r = 0.15$ .



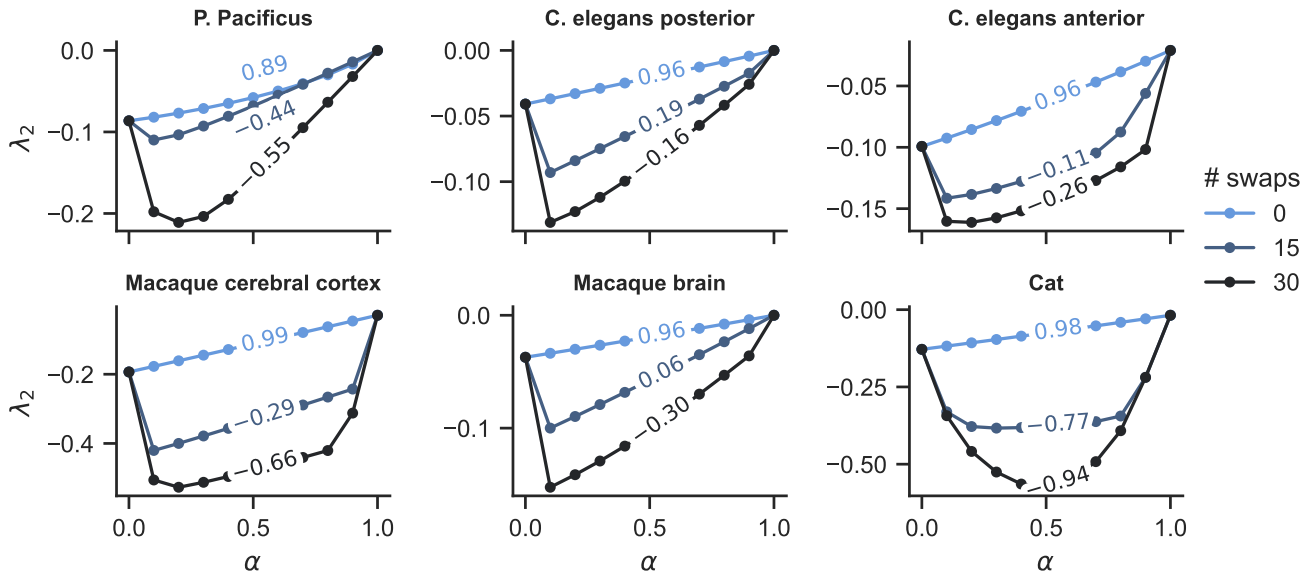
Supplementary Figure S6. **Synchronization stability of hypergraphs constructed from synthetic networks.** Analog of Fig. 5, but for scale-free (BA) networks and small-world (SW) networks. The hypergraphs are constructed in the same way as in Fig. 5. For each value of  $p_s$ , we plot synchronization stability  $\lambda_2$  (averaged over 100 independent realizations) as a function of the control parameter  $\alpha$ . We fix the network size to  $n = 100$  for both classes of networks. The BA networks have a mean degree of  $2m$ , whereas the SW networks have a mean degree of  $m$ . Regardless of the mean degree, the role of higher-order interactions always transitions from impeding synchronization to promoting synchronization as  $p_s$  is increased.



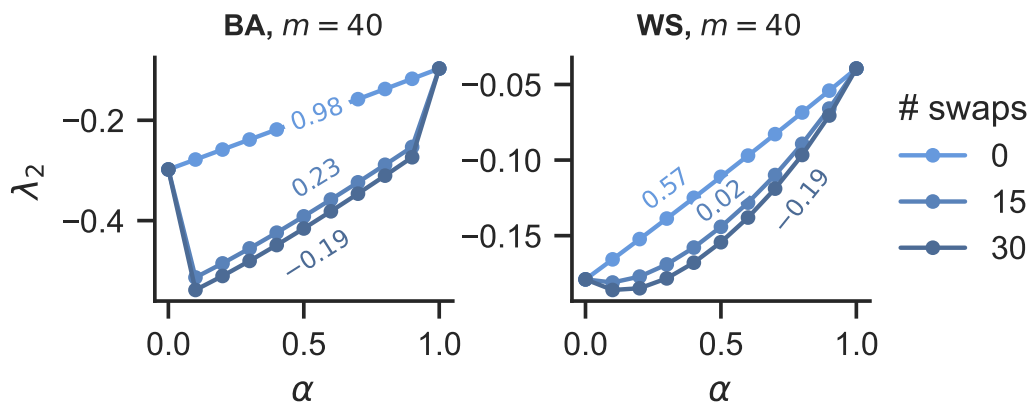
Supplementary Figure S7. **Nonpairwise interactions enhance synchronization in hypergraphs constructed from scale-free (BA) networks and small-world (SW) networks, except when the hypergraph structure is close to being a simplicial complex.** This plot uses the same data as in Supplementary Fig. S6 and is the analogy of Fig. 6 for synthetic networks.



Supplementary Figure S8. **Analog of Fig. 5 based on real-world hypergraphs.** The hypergraphs come from social contacts in a Lyon hospital and a primary school. They are known to be close to being simplicial complexes [21]. From these datasets, we keep hyperedges up to order two and consider the largest connected component. For each value of  $p_s$ , we plot synchronization stability  $\lambda_2$  (averaged over 100 independent realizations) as a function of the control parameter  $\alpha$ . The role of higher-order interactions quickly transitions from impeding synchronization to promoting synchronization as  $p_s$  is increased.



Supplementary Figure S9. **Cross-order degree correlation affects synchronization stability in systems with mixed pairwise and nonpairwise interactions** ( $0 < \alpha < 1$ ). This plot uses the same networks as in Fig. 5 and extends Fig. 7. Curves are colour-coded by the number of pairs of nodes that were selected to swap their 2-simplices memberships: 0, 15, or 30. The resulting degree correlation is indicated on each curve.



Supplementary Figure S10. **Cross-order degree correlation affects synchronization stability in systems with mixed pairwise and nonpairwise interactions** ( $0 < \alpha < 1$ ). The hypergraphs are constructed from scale-free and small-world networks, with the same parameters as in Supplementary Figs. S4 and S5:  $n = 300$ ,  $m = 40$ , and  $p_r = 0.15$ . Curves are colour-coded by the number of pairs of nodes that were selected to swap their 2-simplices memberships: 0, 15, or 30. The resulting cross-order degree correlation is indicated on each curve.